Analysis of Aerodynamic Characteristics of Vertical Axis Wind Turbine (VAWT) Based on Modified Double Multiple Stream Tube Model

Zhicheng Wang[1,2], Jie Zhao[1,*], Md Rayhan Tanvir[2] and Jiexian Mao[1]

[1]*School of Mechanical and Electronic Engineering, East China University of Technology, Nanchang Jiangxi 330013, China*
[2]*Jiangxi Engineering Research Center for New Energy Technology and Equipment, Nanchang Jiangxi 330013, China*
E-mail: 396024135@qq.com
[*]*Corresponding Author*

Received 03 November 2021; Accepted 01 December 2021;
Publication 18 January 2022

Abstract

To further improvement of the aerodynamic performance simulation model accuracy of Vertical Axis Wind Turbine (VAWT), based on the traditional double multi-flow tube theoretical model, the aerodynamic parameters of the airfoil before and after stall are modified by the Lanchester method. Prand model is used to modify the aspect ratio of the airfoil under the condition of the small angle of attack before stall. Viterna Corrigan model is used to modify the aspect ratio, lift and drag coefficients of the airfoil under the stall. And a relaxation factor is introduced to correct the induction factor, also to improve the iterative non-convergence of the simulation under the condition of large tip speed ratio. The simulation results match the experimental data very well. Based on this new aerodynamic performance analysis method, the influence of blade tip speed ratio, blade number, blade chord length,

European Journal of Computational Mechanics, Vol. 30_4–6, 453–480.
doi: 10.13052/ejcm2642-2085.30467

rotor radius, and incoming wind speed on power coefficient and tangential force coefficient is studied, which can provide a reference for the design of aerodynamic performance parameters of the wind turbine.

Keywords: Vertical axis wind turbine, VAWT, theoretical model, aerodynamic characteristics, power coefficient.

1 Introduction

Vertical Axis Wind Turbines (VAWTs) have many advantages, such as simple structure, less noise pollution, multi-directional wind without yaw system, etc. But the commercialization use of VAWT is still not as high as Horizontal Axis Wind Turbines. The main reason is the lack of theoretical research and the late start of technical research. Therefore, the theoretical research on VAWTs is more significant. The theoretical research methods to model the aerodynamic performance of the VAWT impeller mainly include the vortex model based on the potential vortex theory and the flow tube model based on the momentum theorem [1–3].

The flow tube model is widely used in the dynamic performance design of VAWT impeller. Although the vortex model can describe the flow field details effectively, it is not suitable for the calculation of the small speed ratio range. When the impeller is running at a small speed ratio, the blade angle of attack changes greatly, leading-edge separated flow is easy to appear, it is difficult to guarantee its convergence. Moreover, the computation time is too long to meet the requirement of rapid prediction of impeller dynamic performance in engineering design. Based on the propeller theory put forward by researcher Glauert [4], Templin first proposed a single-stream tube model [5] to analyze the aerodynamic performance of wind turbines. Wilson and Lissman [6] put forward the multi-flow tube aerodynamic performance calculation model based on the single-flow tube aerodynamic performance calculation model. Blusseau and Patel [7] calculated the aerodynamic performance of a floating VAWT using a two-way multi-flow tube model, they found that the dynamic response of the wind turbine system would not be affected by the rotational torque. Svorcan et al. [8] analyzed the aerodynamic performance of a small VAWT using a two-way multi-flow tube aerodynamic performance calculation model. The research conclusions were used in the design of VAWTs on top of high-rise buildings in urban areas. Sutherland et al. [9] presented the stream tube model that was helpful to analyze the aerodynamic response of VAWT. Fernández et al. [10] identified the increase of the performance of a VAWT design using the proposed airfoil instead

of the original one has been verified using a double-multiple stream tube model. Paraschivoiu [11] introduced a double-multiple stream tube approach. The model is based on the momentum theory that divides the upstream and downstream stream tubes. The method is shown to be more accurate than its preceding method proposed by Strickland [12], but it still suffers from the difficulty of predicting turbine performance under moderate to high stability conditions. Galih Bangga et al. [13] identified 3D CFD simulations deliver a better agreement with the experimental data but the main behavior of the power curve is reasonably predicted by the 2D CFD simulations.

The effect of dynamic stall is also important for the operation of VAWT. Dynamic stall is an inherent feature of VAWT. There are several methods to simulate the effects of dynamic stall. An overview of dynamic stall models for VAWTs applications can be found in [14, 15]. The amplitude of attack angle increases with the decrease of Tip Speed Ratio (TSR), and there is a dynamic stall at low TSR [16]. Danao La et al. [17] studied the performance of VAWT in steady and unsteady flow field based on the CFD method of Reynolds Average Navier Stokes equation (RANS). The effects of blade stall and fluid reattachment on the performance of wind turbine in unsteady flow fields are discussed in detail. ZHU et al. [18] investigated the different airfoils, various solidity, and architectural configurations also have a great influence on the aerodynamic performance of Building Augmented Straight-Bladed Vertical Axis Wind Turbine (BASB-VAWT). The load of VAWT can be calculated by using the empirical formula model [19] and theoretical model [20]. Buchner et al. [21] studied the dynamic stall phenomenon of VAWT and found the TSR was less than 3, which significantly reduced the power of VAWT. Ma et al. [22] proposed a dynamic stall control scheme for VAWT based on pulsed Dielectric-Barrier-Discharge (DBD) plasma actuation by using Computational Fluid Dynamics (CFD).

In this paper, a theoretical model for the aerodynamic performance of the VAWT is developed based on the double-actuated disk multi-flow tube aerodynamic performance model. This model is also combined with the aerodynamic modification before and after airfoil stall and momentum modification. The model is used to simulate and analyze the aerodynamic characteristics of the VAWT. Moreover, the influence of the number of blades, chord length, radius of the wind wheel on the wind turbine performance is also studied.

2 Theoretical Basis

The calculation model of the aerodynamic performance of the dual-actuating disc multi-flow tube is based on the leaf element momentum theory. This

model divides the wind wheel into two actuating discs, an upper and a lower actuating disc. The two actuating discs correspond to the upper and lower wind flow fields on the rotating surface of the wind wheel respectively. At the same time, the multi-flow tube aerodynamic performance calculation model is used for the upper and lower wind flow fields. According to calculation and analysis, the induction factors in the flow tube in each actuation disk are independent of each other, and the multi-flow tube model of the double actuation disk is shown in Figure 1.

As shown in Figure 1, assuming that V_∞ is the airflow velocity very far from the front end of the wind wheel, V_{au} is the induced velocity of the upper actuating disk of the wind wheel, V_e is the velocity of the airflow after passing through the upper actuating disk element, V_{ad} is the induced velocity of entering the lower actuating disk, and V_w is the distance wind the airflow velocity at a certain distance from the end of the wheel, a_u is the upper actuating disc inducing factor, and a_d is the lower actuating disc inducing factor, then

$$\begin{cases} V_{au} = a_u V_\infty \\ V_e = (2a_u - 1)V_\infty \\ V_{ad} = a_d(2a_u - 1)V_\infty \end{cases} \tag{1}$$

According to the momentum theorem, the thrust coefficients of the upper and lower actuator discs are:

$$\begin{cases} C_{T\mathrm{u}} = 4a_u(1 - a_u) \\ C_{Td} = 4a_d(1 - a_d) \end{cases} \tag{2}$$

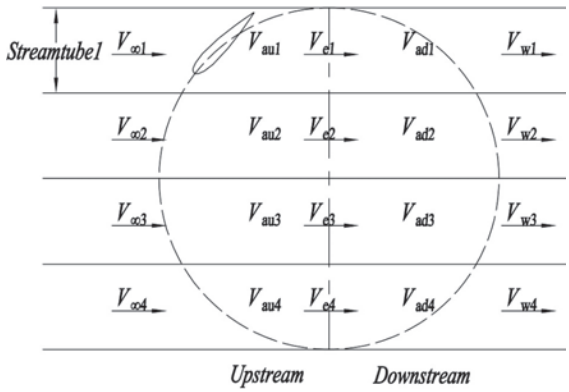

Figure 1 Double disk multiple stream tube model.

According to the leaf element theory, the average thrust coefficients of the upper and lower actuating disks are:

$$\begin{cases} C_{T\mathrm{u}} = \dfrac{Nc}{2\pi R}\dfrac{W_u^2}{V_\infty^2}\sec\theta(C_{nu}\cos\theta - C_{tu}\sin\theta) \\ C_{Td} = \dfrac{Nc}{2\pi R}\dfrac{W_d^2}{V_e^2}\sec\theta(C_{nd}\cos\theta - C_{td}\sin\theta) \end{cases} \tag{3}$$

Where σ is the compactness of the vertical shaft wind turbine wheel; $\Delta\theta$ is the azimuth Angle$^\circ$.

Combining the above formulas, the iterative formulas for the induction factors of the flow tubes of the upper and lower actuation plates are:

$$\begin{cases} 4a_u(1-a_u) = \dfrac{Nc}{2\pi R}\cdot\dfrac{W_u^2}{V_\infty^2}\cdot\sec\theta\cdot(C_{nu}\cos\theta - C_{tu}\sin\theta) \\ 4a_d(1-a_d) = \dfrac{\mathrm{Nc}}{2\pi R}\cdot\dfrac{W_d^2}{V_e^2}\cdot\sec\theta\cdot(C_{nd}\cos\theta - C_{td}\sin\theta) \end{cases} \tag{4}$$

The relevant parameters of the upper actuation plate are:

$$\begin{cases} \lambda_u = \dfrac{\omega R}{V_u} \\ W_u = \sqrt{(V_u(\lambda_u + \cos\theta))^2 + (V_u\sin\theta)^2} \\ \alpha_u = \sin^{-1}\left(\dfrac{V_u\sin\theta}{W_u}\right) \\ Re_u = \dfrac{W_u c}{\nu} \\ C_{nu} = C_{lu}\cos\alpha_u + C_{du}\sin\alpha_u \\ C_{tu} = C_{lu}\sin\alpha_u - C_{du}\cos\alpha_u \\ T_{su}(\theta) = \dfrac{1}{2}\rho c R W_u^2 C_{tu}\cdot\Delta h \\ \overline{T_u} = \dfrac{N}{2\pi}\displaystyle\int_{-\frac{\pi}{2}}^{\frac{\pi}{2}} T_{su}(\theta) \\ C_{qu} = \dfrac{\overline{T_u}}{\frac{1}{2}\rho A_u V_\infty^2} \\ C_{P1} = C_{qu}\lambda \end{cases} \tag{5}$$

The relevant parameters of the lower actuation plate are:

$$\begin{cases} \lambda_d = \dfrac{\omega R}{V_d} \\ W_d = \sqrt{(V_d(\lambda_d + \cos\theta))^2 + (V_d \sin\theta)^2} \\ \alpha_d = \sin^{-1}\left(\dfrac{V_d \sin\theta}{W_d}\right) \\ Re_d = \dfrac{W_d c}{\nu} \\ C_{nd} = C_{ld}\cos\alpha_d + C_{dd}\sin\alpha_d \\ C_{td} = C_{ld}\sin\alpha_d - C_{dd}\cos\alpha_d \\ T_{sd}(\theta) = \dfrac{1}{2}\rho c R W_d^2 C_{td} \cdot \Delta h \\ \overline{T_d} = \dfrac{N}{2\pi}\displaystyle\int_{\frac{\pi}{2}}^{\frac{3\pi}{2}} T_{sd}(\theta) \\ C_{qd} = \dfrac{\overline{T_D}}{\frac{1}{2}\rho A_d V_\infty^2} \\ C_{P2} = C_{qd}\lambda \end{cases} \tag{6}$$

From the above, we can see the wind energy utilization coefficient C_P of the entire VAWT is:

$$C_P = C_{P1} + C_{P2} \tag{7}$$

It is known that most airfoil aerodynamic parameters are obtained under the condition that the aspect ratio is close to infinity, and the aspect ratio of the blade is relatively small during design and application, which leads to errors between the data. The Lanchester-Prand modified model is used here to modify the aspect ratio of the airfoil before the stall and the angle of attack is small.

$$C_l = C_l' \tag{8}$$

$$C_d = C_d' + \frac{C_l^2}{\pi\tau} \tag{9}$$

$$\alpha = \alpha' + \frac{C_l}{\pi\tau} \tag{10}$$

in which C_l' is the lift coefficient before correction; C_d' is the drag coefficient before correction; α' is the corrected front angle of attack; τ is the aspect ratio, $\tau = H/c$.

When the angle of attack of the airfoil exceeds a certain angle, there will be delayed response of lift coefficient and drag coefficient, and the data obtained in this case is quite different from the experimental data of the airfoil at rest. In this paper, Viterna-Corrignan model [23] is used to modify the aspect ratio, lift (C_l) and drag (C_d) coefficients of the airfoil at stall.

$$C_l = \frac{1.11 + 0.018\tau}{2} \sin 2\alpha \left[C_{ls} - (1.11 + 0.018\tau) \sin \alpha_s \cos \alpha_s\right] \times \frac{\sin \alpha_s \cos^2 \alpha}{\cos^2 \alpha_s \sin \alpha} \tag{11}$$

$$C_d = (1.11 + 0.018\tau) \sin^2 \alpha + \left[C_{ds} - \frac{(1.11 + 0.018\tau) \sin^2 \alpha_s}{\cos \alpha_s}\right] \cos \alpha \tag{12}$$

In which α_s is the stall angle of attack; C_{ls} is the lift coefficient at stall angle of attack; C_{ds} is the drag coefficient at stall angle of attack.

According to the momentum theory, the higher the weakening degree of the flow through the blade, the higher the effect of thrust on the blade. When the induction factor is used, the effect of thrust on the blade is gradually reduced, which leads to the inconsistency between the calculation model and the actual situation. Glauert [4] proposed an empirical formula to modify the thrust coefficient in the range of induction factor from 0.4 to 1.0 in the aerodynamic performance calculation model, making the model more closed to the actual situation. Then the corrected thrust coefficient of the upper and lower actuating discs of the wind turbine is as follows:

$$\begin{cases} C_T = 4a(1-a) & 0 < a < 0.4 \\ C_T = 4a\left[1 - \dfrac{1}{4}a(5-3a)\right] & 0.4 < a < 1.0 \end{cases} \tag{13}$$

In the case of large tip velocity, it is possible that the iteration will not converge if the Glauert [4] correction is used. A relaxation factor is introduced here, and the newly obtained induction factor is corrected by the relaxation factor [24].

$$a_n = wa_n + (1-w)a_o \tag{14}$$

In which w is the relaxation factor, $w = 0.3$; a_n is the corrected induction factor; a_o is the uncorrected induction factor.

3 Establishment of Theoretical Model for Aerodynamic Performance of VAWT

Through the VAWT aerodynamic performance theoretical model, the program of the aerodynamic performance theoretical model is compiled based on MATLAB. The program is divided into two parts: the processing of airfoil aerodynamic parameters and the iterative solution of the induction factors in the upper and lower actuated disk flow tubes.

The process of airfoil aerodynamic parameters is as follows:

(1) Obtain and correct the original data of C_l and C_d of the initial airfoil with the angle of attack in the range of $0 \sim 90°$;
(2) Interpolate the Reynolds number and the angle of attack to obtain the corresponding airfoil aerodynamic parameters C_l and C_d;
(3) Within a certain range of angle of attack, determine the tangential force coefficient C_t and the normal force coefficient C_n through the airfoil aerodynamic parameter correction data, and provide the corresponding airfoil aerodynamic parameter data support for the iterative solution process of the induction factor.

In order to improve the accuracy of the calculation results of the model, this paper discretizes and calculates the angle of one rotation of the wind wheel in the model. Take 5 as an azimuth angle, divide the rotation position of the wind wheel into 72 equally, and calculate the aerodynamic performance of each azimuth angle. The specific process is as follows:

(a) Assuming that the initial induction factor $a_0 = 1$ in each flow tube in the moving plate, we can get $V_a = V_\infty$;
(b) Given the value of θ, get the corresponding relative velocity W, angle of attack α, and local Reynolds number Re from Equation (5);
(c) Determine the tangential force coefficient C_t and the normal force coefficient C_n of the airfoil according to the local Reynolds number Re and the angle of attack α;
(d) Substituting the above data into Equation (4) can obtain new inducing factors a_{new};
(e) When $a_{new} - a_u < 0.001$, the iteration stops and the value of the new induction factor a_{new} is output;
(f) Then the power coefficient C_P of the actuation plate can be calculated.

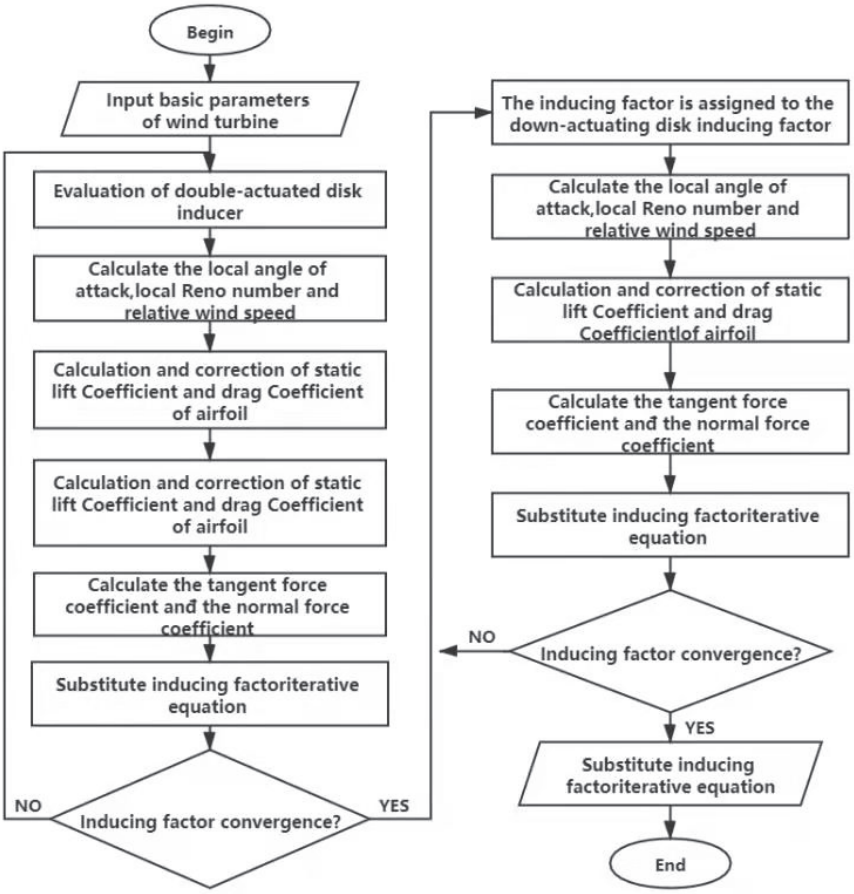

Figure 2 Program flow chart.

Based on the above content, this paper compiles the MATLAB program of the VAWT aerodynamic performance theoretical analysis model. The program running process is shown in Figure 2.

4 Simulation Analysis on Aerodynamic Performance of VAWT

4.1 Aerodynamic Performance Analysis of VAWT

Compared with the traditional dual multi-flow management theory model, the theoretical model of wind turbine aerodynamic performance proposed in

Table 1 Main geometrical parameters of wind rotor

Parameter	Value
Rotor diameter	6.0 m
Rotor height	6.0 m
Blade length	6.0 m
Blade chord (constant)	0.2 m
Blade airfoil	NACA 0015
Numbers of blades	2
Rotor ground clearance	3 m

Source: [26].

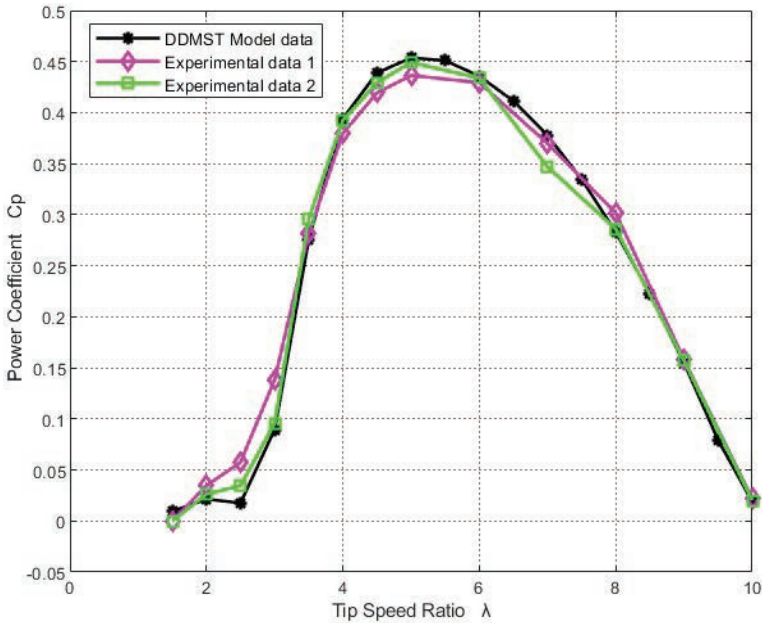

Figure 3 Comparison of model data and experimental data.

this paper adds the correction of aerodynamic parameters before and after the airfoil stall. Therefore, the program of the theoretical model compiled in this paper is referred to as Double Disk Multiple Stream Tube (DDMST). In this paper, the power coefficient curve (black line Figure 3) was computed with DDMST, also compared with two groups of experiment data from I Paraschivoiu et al. [25]. The rotor having the main geometrical characteristics given in Table 1.

Table 2 Main geometrical parameters of wind rotor

Parameter	Value
Incoming wind speed V_o (m/s)	10
Airfoil model	NACA 0018
Airfoil chord c (m)	0.15
Wind wheel radius R (m)	2.5
Number of blades N	4
Wind wheel height L (m)	5

From Figure 3, it can be found that the calculated value of the DDMST model and the experimental value is consistent with the TSR range when the power coefficient value is large, and both are in the range of TSR from 3.5 to 8.5; both are at the corresponding highest power coefficient. The TSR at the time is the same, and the maximum power coefficient value calculated by the model is slightly larger than the experimental value. The relationship curve of the calculated value of the model is consistent with the relationship curve of the experimental value. Therefore, the theoretical analysis model of wind turbine aerodynamic performance constructed in this paper can predict the aerodynamic performance of the VAWT rotor more accurately.

Based on the above results. This study was carried by a set of wind rotor model parameters shown in Table 2.

(1) Power Coefficient

The performance of the power coefficient was computed with DDMST. The relationship change curve between the power coefficient and the TSR is obtained through calculation, as shown in Figure 4.

The curves of the total power coefficient, the power coefficient of the upper actuation disk, and the power coefficient of the lower actuation disk are similar to the parabola (Figure 4). When the TSR becomes larger, the three first increase and then decrease. This result meet the law that the Power Coefficient decreasing with the increase of TSR. When the TSR is greater than 3.5, the lower actuation disk rotor is disturbed by the upper actuation disk rotor during operation. Under the condition of low TSR, the power coefficient of the upper actuating disc is greater than the coefficient of the lower actuating disc. The possible cause is the dynamic stall effect. The stall model only weakens the dynamic stall effect but does not eliminate it. The total power coefficient reaches its maximum value when the TSR is 4, and the maximum value is 0.454. Here, the rotor speed is about 16 rad/s.

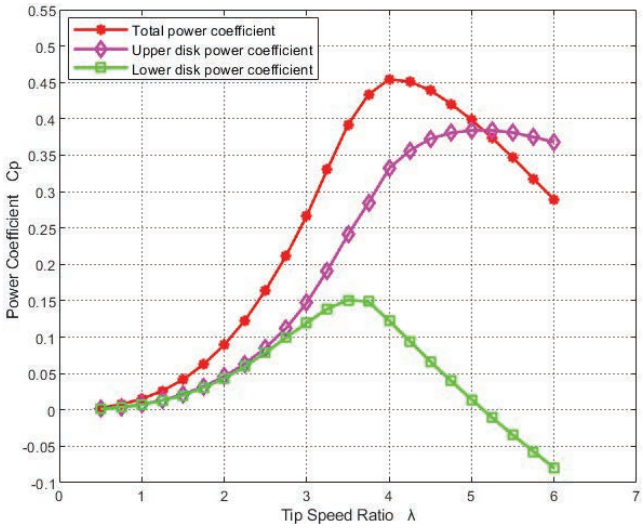

Figure 4 Power coefficient curves.

(2) Tangential Force Coefficient

According to the leaf element theory, the tangential force of the blade drives the rotation of the wind wheel, and the change of the aerodynamic load of the blade changes with the change of the tangential force, and the change of the tangential force can be expressed by the change of the tangential force coefficient.

Keep other parameters unchanged, set the simulated wind wheel speed to 16 rad/s, and study the change of the tangential force coefficient of a single blade during one rotation of the wind wheel under the condition of the incoming wind speed of 6 to 12. The simulation result is shown in Figure 5.

During the blade rotation process (Figure 5), most of the tangential force coefficients are positive. Under different wind speeds below 10, the tangential force coefficient curves have similar trends, and their values vary with it becomes larger as the wind speed increases. After the wind speed reaches or exceeds 10, the tangential force coefficient in the upper actuating disk area rises, then drops, then rises, and then falls. The main reason for this phenomenon is that when the wind wheel speed is constant, the wind speed increases, and the blades The TSR decreases, which in turn increases the blade angle of attack. When the blade is at a high angle of attack, a stall will occur, resulting in a decrease in the lift coefficient of the airfoil and a decrease in the tangential force coefficient.

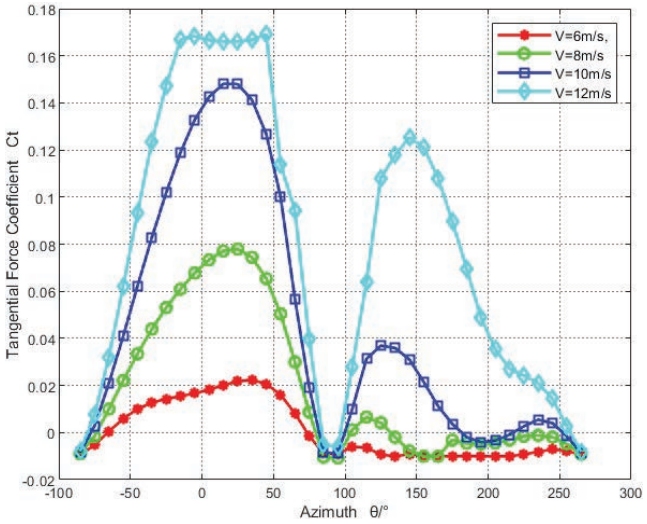

Figure 5 Tangential force coefficient curves at different wind speeds.

4.2 Influence of Wind Turbine Parameters on Wind Turbine Performance

The performance of the wind turbine can be evaluated by the power coefficient, and the influence of the wind turbine parameters on the performance of the wind turbine is studied through the theoretical analysis model of the aerodynamic performance of the wind turbine.

(1) Effect of the Blade Numbers on Wind Turbine Performance

Keep other parameters unchanged, study the effect of the number of blades on the performance of the wind turbine when the number of blades is 2 to 6, and the simulation results are shown in Figure 6.

Each relationship curve in the Figure 6 shows that when the TSR continues to increase, the power coefficient first increases and then decreases. When the blade TSR is less than 1, the wind turbine power coefficient is not affected by the increase or decrease of the number of blades, but in the process of increasing the blade TSR, it is more and more affected by the number of blades. In the process of increasing the number of blades from 2 to 6 blades, the peak value of the wind turbine power coefficient first increases and then decreases, and the TSR corresponding to the peak value also decreases. The blade TSR range for the wind turbine to maintain a higher power coefficient becomes narrower and the overall power coefficient curve tends to move to

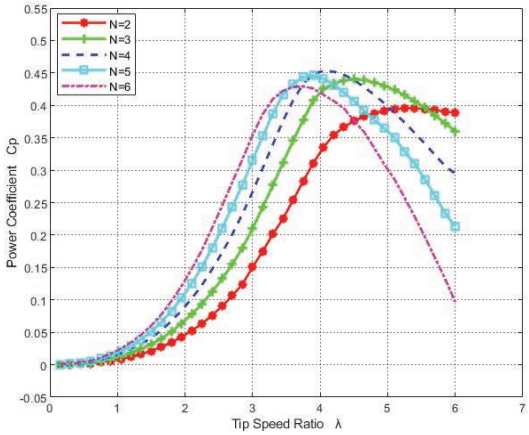

Figure 6 Influence of blade number on power coefficient.

the left, indicating that the wind turbine's self-starting characteristics have improved.

(2) Effect of Blade Chord on Wind Turbine Performance

Keep other parameters unchanged, and study the effect of the chord length on the performance of the wind turbine when the chord length is 0.15∼0.35. The simulation result is shown in Figure 7.

As the chord length increases from 0.15 to 0.35, the peak value of the wind turbine power coefficient first increases and then decreases, and the peak speed ratio corresponding to the peak value also decreases (Figure 7). The blade TSR range for the wind turbine to maintain a higher power coefficient change. i.e., the power coefficient curve generally tends to move to the left. Besides, the solidity of the wind wheel increases with the increase of the chord length of the blades, causing the blades to interact with each other to interfere with the flow field, which seriously affects the wind wheel to obtain energy from the airflow. Therefore, the peak value of the power coefficient increases with the further increase of the chord length. i.e., if the chord length is too small, the instantaneous torque on the blade will decrease and the power coefficient will also decrease.

(3) Influence of Wind Wheel Radius on Wind Wheel Performance

Keep other parameters unchanged, study the influence of the wind wheel radius on the performance of the wind turbine when the radius of the wind wheel is 2 to 4, and the simulation results are shown in Figure 8.

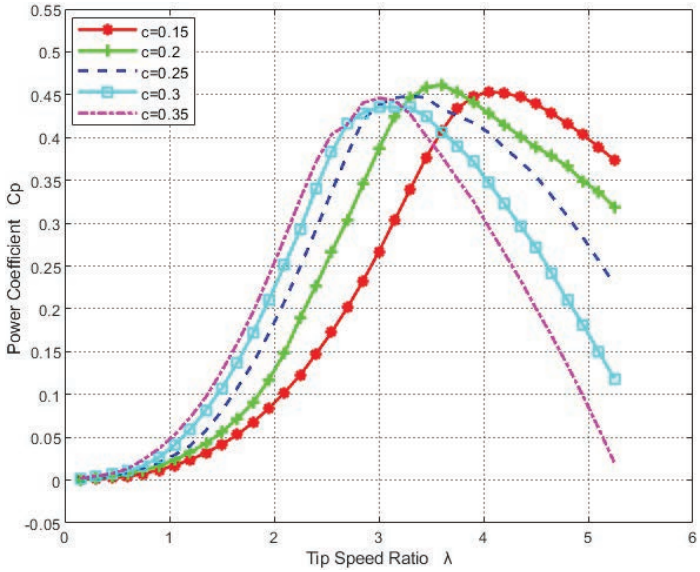

Figure 7 Influence of blade chord length on power coefficient.

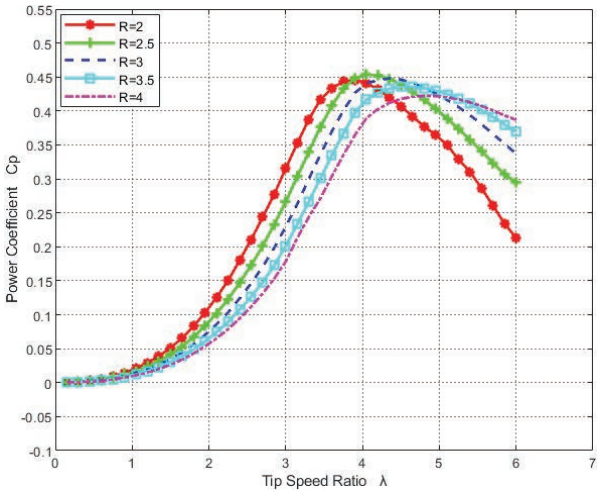

Figure 8 Influence of wind rotor radius on power coefficient.

In the process of increasing the radius from 2 m to 4 m, the peak value of the wind turbine's power coefficient first increases and then decreases (Figure 8). The peak value corresponds to an increase in the TSR, and the wind turbine maintains a higher power factor TSR as the range becomes

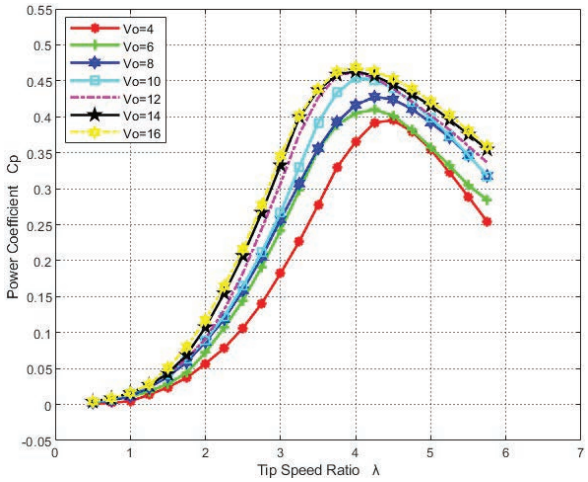

Figure 9 Influence of wind speed on power coefficient.

wider, the power coefficient curve tends to move to the right as a whole, and the self-starting performance of the wind turbine decreases. This is because the solidity of the wind wheel decreases as the radius of the wind wheel increases, and the influence of the blades interacting and interfering with the flow field becomes weaker, the effective angle of attack of the airfoil increases, the lift increases, and the instantaneous torque of the blade becomes larger, resulting in a decrease in the self-starting performance of the wind turbine.

4.3 Influence of Incoming Wind Speed on Wind Turbine Performance

Under the conditions of 4 blades, wind wheel radius 2.5 m, blade chord length 0.15 m, wind wheel height 5 m, airfoil NACA0018, etc., the effect of incoming wind speeds from 4 m/s to 16 m/s on the performance of the wind turbine is studied. The simulation results are shown in Figure 9.

Each relationship curve shows that when the TSR continues to increase, the wind turbine power coefficient first increases and then decreases (Figure 9). When the TSR is less than 1, the wind turbine power coefficient is not affected by the increase or decrease of the incoming wind speed. During the increase of the blade TSR, the wind turbine power coefficient is more and more affected by the incoming wind speed. In the process of increasing the incoming wind speed from 4 m/s to 16 m/s, the peak value of the wind

turbine's power coefficient increases, and the peak value corresponds to a decrease in the TSR. The range of the TSR for the wind turbine to maintain a higher power coefficient becomes wider. But when the incoming wind speed exceeds 10 m/s, the influence on the power coefficient gradually becomes weaker.

5 Design of Optimization Algorithm for Wind Turbine Parameters Based on Improved Particle Swarm Optimization

5.1 Construction of Improved Particle Swarm Optimization Algorithm

Particle Swarm Optimization (PSO) [26] is a kind of global stochastic optimization algorithm. The basic principle is: suppose there is a D-dimensional search space for optimization problems, which contains a swarm of N particles. In this swarm, The State of the I particle is expressed in terms of its position state and velocity state. The positional state is recorded as $X_i = (x_{i1}, x_{i2}, \ldots, x_{iD})$, the velocity state is recorded as $V_i = (v_{i1}, v_{i2}, \ldots, v_{iD})$. P_{best} is the best position found by particle i, recorded as $P_{best} = (p_{i1}, p_{i2}, \ldots, p_{iD})$. And the best solution found by all individuals of the whole particle swarm is called global extremum, recorded as $G_{best} = (P_{best\ 1}, P_{best\ 2}, \ldots P_{best\ D})$.

In this paper, an improved PSO algorithm with inertia weight is used. This algorithm updates the flight speed and position of particles within the swarm. The formula is as follows:

$$v_{ij}(t+1) = \omega \cdot v_{ij}(t) + c_1 \cdot r_1(t) \cdot (pbest_{ij}(t) - x_{ij}(t)) + c_2 \cdot r_2(t) \cdot (gbest_j(t) - x_{ij}(t)) \tag{15}$$

$$x_{ij}(t+1) = x_{ij}(t) + v_{ij}(t+1) \tag{16}$$

The inertia weight represents the ability of the individual particles in the swarm to maintain the previous flight speed, and the search ability of the population is directly affected by it. The smaller the inertia weight, the stronger the local space searching ability and the weaker the space searching ability of PSO Algorithm.

In Equation (17) the inertia weight is:

$$\omega(t) = \omega_{\min} + \frac{\omega_{\max} - \omega_{\min}}{t_{\max}} \cdot (t_{\max} - t) \tag{17}$$

Where t is the number of current iterations; tmax is maximum number of iterations of the algorithm; $\omega_{\max}$ is the maximum inertia weight factor; $\omega_{\min}$ is the minimum inertia weight factor.

The fixed value of the learning factor of the basic PSO algorithm is easy to cause the poor convergence effect in the whole space, Ratnaweera et al. studied the influence of learning factors on PSO algorithm, and improved the learning factors, the formula is as follows:

$$\begin{cases} c_1 = (c_{1f} - c_{1i}) \cdot \dfrac{t}{t_{\max}} + c_{1i} \\ c_2 = (c_{2f} - c_{2i}) \cdot \dfrac{t}{t_{\max}} + c_{2i} \end{cases} \tag{18}$$

Where $c_{1i} = 2.5$, $c_{1f} = 0.5$, $c_{2i} = 1$, $c_{2f} = 2.25$. Related research results show this method strengthens the space searching ability of PSO, speeds up the convergence speed of PSO, and converges well at the end of searching and finds the best solution in the whole space.

5.2 Algorithm Realization of Optimization Model

(1) Objective function of optimization model

The performance of the wind turbine can be evaluated by the annual energy output of it. Taking into account the probability distribution of wind speed, the annual average output power of the wind turbine is obtained by taking the average value of the output power of it from the cut-in wind speed to the stopped speed. The optimized design target can be determined as the annual average output power of the largest wind turbine. According to the fact that there is no constant wind speed in the wind farm, after introducing the condition of the probability distribution of wind speed, the actual output of the wind turbine in life can be better displayed in the annual average output power of the wind turbine. Then the objective function of the optimization model can be defined as:

$$f(x) = \overline{APE} = \int_{V_{in}}^{V_{out}} f(V) \cdot P(V) dV \tag{19}$$

Where $\overline{APE}$ (KW) is the Annual average output power of wind turbine,V_{in} (m/s) is the Starting speed, V_{out} is the stopped speed, $f(V)$ is the Weibull distribution function of wind speed, $P(V)$ (KW) is the output power.

The output power $P(V)$ is:

$$P(V) = \begin{cases} 0 & 0 \le V \le V_{in} \\ P(V) & V_{in} \le V \le V_{out} \\ P(V_t) & V_t \le V \le V_{out} \\ 0 & V_{out} \le V \end{cases} \tag{20}$$

Where V_t (m/s) is Rated wind speed, $P(V_t)$ (KW) is rated power.

(2) Constraints of optimization model

In this paper, the improved PSO algorithm with inertia weight can determine the selection range of design variables, according to the influence law of wind turbine parameters on its performance shown in the DDMST program. So as to avoid selecting the wrong design variable value, and further improve the efficiency of the optimization program. Each independent particle in the PSO algorithm searches for the best solution under the corresponding constraint conditions, and then determines the best solution in the whole space and the best solution in the local space of the objective function of the optimization model. The constraint equations adopted in this optimization model are as follows:

$$\begin{cases} N_{\min} \le N \le N_{\max} \\ R_{\min} \le R \le R_{\max} \\ V_{t\min} \le V_t \le V_{t\max} \\ c_{\min} \le c \le c_{\max} \end{cases} \tag{21}$$

Where N is the number of blades (the value is an integer), $N_{\min}$ is the minimum number of blades, $N_{\max}$ is the maximum number of blades, R is the radius of the wind wheel, $R_{\min}$ is the minimum wind wheel radius, $R_{\max}$ is the maximum wind wheel radius, V_t is the rated wind speed, $V_{t\min}$ is the minimum rated wind speed, $V_{t\max}$ is the maximum rated wind speed, c is the blade chord length, $c_{\min}$ is the minimum blade chord length, $c_{\max}$ is the maximum blade chord length.

(3) Optimized program design

Based on the calculation model of aerodynamic performance of multi-flow tube with double-actuated disk, by using the improved PSO algorithm as the core algorithm to calculate the objective function value. The program flow chart of the optimization algorithm is shown in Figure 10.

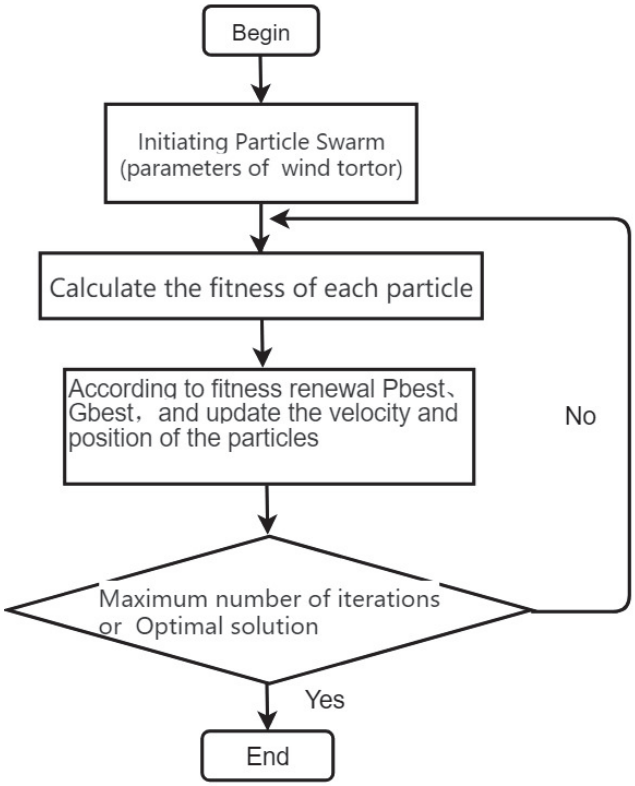

Figure 10 Algorithm flow chart.

5.3 Case Analysis of Wind Rotor Parameters Optimization

(1) Parameters optimization of wind rotor

The design variables of this optimization are the number of blades of the wind rotor (the number of blades is integer), the radius of the wind rotor, the rated wind speed and the chord length of the blades. The optimization objective function is the annual average output power of the turbine, as shown in formula (19). The constraints of the optimization are as follows:

$$\begin{cases} 2 \leq N \leq 5 \\ 2 \leq R \leq 4 \\ 8 \leq V_t \leq 12 \\ 0.15 \leq c \leq 0.4 \end{cases} \tag{22}$$

Table 3 The parameters of wind rotor

Parameters	Initial Design Value	Optimized Design Value
Radius(m)	2.5	2.275
Hight(m)	5	5.49
Chord length (m)	0.15	0.25
Number of blades	4	5
Rated speed (m/s)	10	11.3
Annual average output power (***KW***)	3.5976	4.1480
Air density (kg/m^3)	1.225	1.225
Cut-in wind speed (m/s)	3.5	3.5
Stopped speed (m/s)	25	25

(2) Optimization result analysis

An improved PSO algorithm with inertia weight is used to calculate the optimal objective function under the corresponding constraints. The parameters before and after optimization are shown in Table 3.

Table 1 shows the average output power of the optimized design parameters of the wind rotor is 4.1480 KW, and the initial is 3.5976 KW, the power output of the former is 15.30% higher than that of the latter. It can be concluded that the average output power of the wind turbine increases significantly, the total power output of the wind turbine increases correspondingly after the optimal design with the specific wind field as the primary condition. The structural diagram of the wind rotor before and after optimization is shown in Figure 11.

The structure of the optimized wind rotor has changed with number of blades increased to five (Figure 11), the chord length of blades increased to 0.25 m, the length of blades increased to 5.49 m, and the radius of the blades decreased to 2.275 m. The power coefficient curves before and after optimization are shown in Figure 12.

As per Figure 12, the peak value of the power coefficient of the optimized turbine moves to the direction of low blade TSR, and its self-starting ability is enhanced obviously. When the TSR is less than 3.5, the power coefficient of the optimized turbine is higher than that of the initial one, and the ability of the rotor to absorb wind energy is enhanced. On the other hand, When the TSR is more than 3.5, the optimized power coefficient is lower than that before optimization. This means the ability of the optimized wind turbine to absorb wind energy is weaker than that of the optimized one in the range of high TSR. This optimization is carried out for a specific wind field, where the

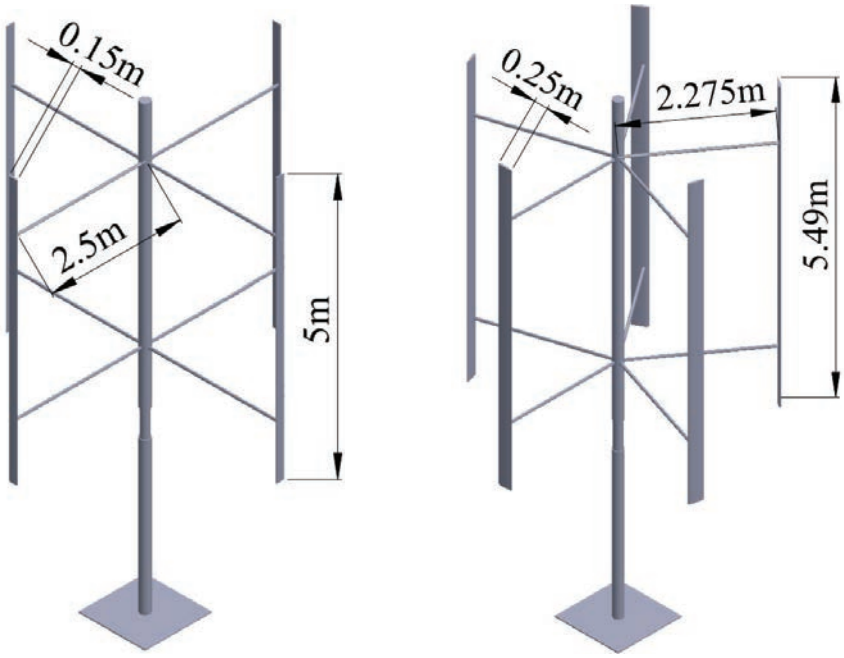

a. Pre-optimization wind rotor b. Optimized wind rotor

Figure 11 Schematic diagram of wind rotor structure.

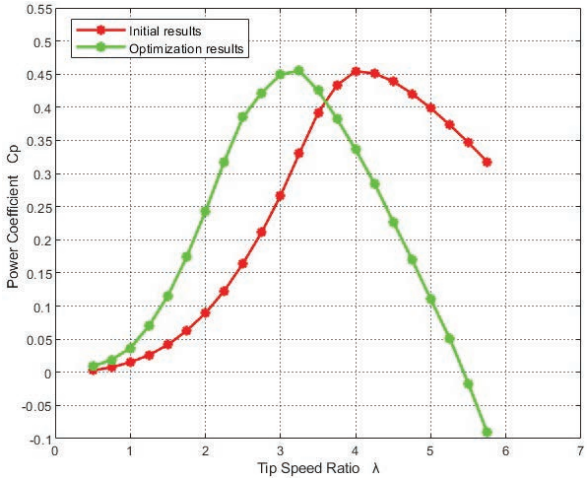

Figure 12 Power coefficient comparison of wind rotor before and after optimization.

annual average value of wind speed is about 8.55 m/s. The optimized turbine is more suitable for the wind field under this wind speed condition.

6 Conclusion

In this paper, a theoretical analysis model of the aerodynamic performance of the wind turbine is established based on the basic theory of the VAWT and the dual-actuating disc multi-flow tube model. The MATLAB program of the model is used to study the aerodynamic performance of the wind turbine and simulate and analyze the impact of related parameters on the performance of the wind turbine influences. The main conclusions are as follows:

(1) The theoretical model of the aerodynamic performance of the wind turbine was solved, and a set of experimental data was used to verify the accuracy of the theoretical model of the aerodynamic performance of the wind turbine.
(2) The change of the tangential force coefficient of a single blade during one rotation of the wind wheel under the same rotating speed and different incoming wind speeds is analyzed. The tangential force coefficient increases as the wind speed increases, but when the wind speed exceeds a certain value, the tangential force coefficient curve in the upper actuation disk area will fluctuate greatly due to the stall phenomenon of the blade at a large angle of attack.
(3) The influence of wind turbine blade number, chord length, wind turbine radius, airfoil, and other wind turbine parameters as well as incoming wind speed on wind turbine performance is analyzed. Through the analysis, it can be known that the changes of the wind turbine parameters and the value of the incoming wind speed will affect the power coefficient of the wind turbine. So, it is more important to select a reasonable parameter range to improve the performance of the wind turbine.
(4) Based on an improved PSO algorithm with inertia weight, an optimization model of wind turbine parameters is constructed by combining the Weibull distribution model of the working state and wind speed of the wind turbine. Then an intelligent optimization algorithm of wind turbine parameters is established by the optimization model, the optimization results show that the annual average output power of the optimized wind turbine is increased by 15.30%.

Acknowledgements

This article is supported by the National Natural Science Foundation Project (Grant No. 51567001), Science and Technology Planning Project (No. 20181BBE58006) Founded by Jiangxi Province, and Science and Technology Cooperation Project (No. 20212BDH80008) – "Belt and Road Initiatives" China-Africa Science and technology cooperation.

References

[1] Trickland JH. The Darrieus Turbine: A Performance Prediction Using Multiple Stream Tubes[J]. Sandia Laboratories Report SAND 75-0431, 1975.

[2] Paraschivoiu I. Double-multiple Stream Tube Model for Darrieus Wind Turbines[J]. Second DOE/NASA wind, 1976.

[3] Strickland JH, Webster BT, Nguyen T. A vortex model of the Darrieus turbine: an analytical and experimental study[J]. Trans ASME J Fluids Eng 1979(101):500–504.

[4] Glauert H. Airplane propellers[M]//Aerodynamic theory. Spring Berlin Heidelberg, 1935:169–360.

[5] Templin RJ. Aerodynamic Performance Theory for the Nrc Vertical-Axis Wind Turbine[J]. NASA STI/Recon Technical Report N, 1974, 76:16618.

[6] Wilson RE, Lissaman PBS. Applied aerodynamics of wind power machines[R]. Oregon State Univ., Corvallis (USA), 1974.

[7] Blusseau P, Patel MH. Gyroscopic effects on a large vertical axis wind turbine mounted on a floating structure[J]. Renewable Energy, 2012, 46:31–42.

[8] Svorcan J, Stupar S, Komarov D, Peković O, Kostić I. Aerodynamic design and analysis of a small-scale vertical axis wind turbine[J]. Journal of Mechanical Science & Technology, 2013, 27(8): 2367–2373.

[9] Sutherland, HJ, Berg, DE, Ashwill, TD. A Retrospective of VAWT Technology; Sandia Report, SAND 2012-0304; Sandia National Laboratories: Albuquerque, NM, USA, January 2012.

[10] Meana-Fernández, A, Díaz-Artos, L, Fernández Oro, JM, Velarde-Suárez S. An optimized airfoil geometry for vertical-axis wind turbine applications[J]. International Journal of Green Energy. 2020.01.16: 2–15.

[11] Ion Paraschivoiu. Double-multiple streamtube model for darrieus in turbines. Second DOE/NASA Wind Turbines Dynamics Workshop. 1981,1:19–25.

[12] Strickland JH, Webster B, Nguyen T. A vortex model of the darrieus turbine: an analytical and experimental study. Journal of Fluids Engineering 1979; 101(4):500–505.

[13] Galih Bangga, Amgad Dessoky, Thorsten Lutz and Ewald Krämer. Improved Double-Multiple-Streamtube approach for H-Darrieus vertical axis wind turbine computations[J]. Energy. 2019.06.

[14] Pereira, R. Validating the Beddoes–Leishman Dynamic Stall Model in the Horizontal Axis Wind Turbine Environment. MS.c. Thesis, Department of Control and Operations, Delft University of Technology, Delft, The Netherlands, 2010.

[15] Ferreira, CJS, van Zuijlen, A, Bijl, H, van Bussel, G, van Kuik, G. Simulating dynamic stall in a two-dimensional vertical-axis wind turbine: Verification and validation with particle image velocimetry data. Wind Energy 2009, 13, 1–17.

[16] Ferreira, CJS, van Zuijlen, A, Bijl, H, van Bussel, G, van Kuik, G. Simulating dynamic stall in a two-dimensional vertical-axis wind turbine: Verification and validation with particle image velocimetry data. Wind Energy 2009, 13, 1–17.

[17] Danao LA, Edwards J, Eboibi O, Howell R, et al. A numerical investigation into the influence of unsteady wind on the performance and aerodynamics of a vertical axis wind turbine. Appl Energy 2014;116:111–124.

[18] Haitian Zhu, Wenxing Hao, Chun Li, and Qinwei Ding. Numerical investigation on the effects of different wind directions, solidity, airfoils, and building configurations on the aerodynamic performance of building augmented vertical axis wind turbines. [J]. International Journal of Green Energy. 2019, 16, 1216–1230.

[19] Christian, M, Christophe, L, Ion, P. Appropriate Dynamic-Stall Models for Performance Predictions of VAWTs with NLF Blades.[J]. Rotating Mach. 1998, 4, 129–139.

[20] Zuo, W, Wang, X, Kang, S. Numerical simulations on the wake effect of H-type vertical axis wind turbines.[J]. Energy. 2016, 106, 691–700.

[21] Buchner, AJ, Soria, J, Honnery, D, Smits, AJ. Dynamic stall in vertical axis wind turbines: Comparing experiments and computations. J. Wind Engrgy. 2015, 146, 163–171.

[22] Lu Ma, Xiaodong Wang, Jian Zhu and Shun Kang. Dynamic Stall of a Vertical-Axis Wind Turbine and Its Control Using Plasma Actuation. [J]. Energies 2019, 12, 3738–3756.
[23] Viterna LA, Corrigan R D. Fix pitch rotor performance of large horizontal axis wind turbines[J]. Large Horizontal-Axis Wind Turbines, 1982, 1:69–85.
[24] Mcintosh SC, Babinsky H, Bertényi T. Convergence Failure and Stall Hysteresis in Actuator-Disk Momentum Models Applied to Vertical Axis Wind Turbines[J]. Journal of Solar Energy Engineering, 2009, 131(3): 376–385.
[25] I. paraschivoiu, O. Trifu, and Saeed F. H- Darrieus wind turbine with blade pitch control[J]. International Journal of Rotating Machinery, 2009 (2009).
[26] Gerhard Venter, Sobieszczanski-Sobieski Jaroslaw. Particle Swarm Optimization[J]. AIAA Journal, 2002, 41(8): 129–132.

Biographies

Zhicheng Wang is a doctor of China Academy of Space Technology. He is a supervisor of master degree, and he has got a visiting scholar of Florida Institute of Technology. His research areas are: mechatronics engineering, New Energy Science and technology. Over the past five years, he has presided over and participated in more than 10 scientific research projects at the national level, provincial and ministerial levels, obtained more than 60 items of various intellectual property rights such as patents and soft works. Based on the transformation and application of scientific research achievements, “Electrostatic atomization series”, “Air energy series”, “Solar energy series” equipment and cloud intelligent management platform have been developed with independent intellectual property rights, and extended to countries and regions along the Belt and Road Initiatives.

Jie Zhao is a lecturer at the electronic engineering of the east China University of Technology. She is mainly engaged in research in the fields of new energy technology application and mechanical engineering. She participate in 4 national, provincial and ministerial-level research projects and has got patents, soft written and other types of intellectual property rights more than 20.

Md Rayhan Tanvir completed his Master degree in 2016. He studied in Electrical Engineering with a major on Power Systems. During his study, he has done a project on renewable energy control systems and involved in several projects afterwards when he started his career in East China University of Technology as a lecturer. His is deeply focused on improving power electronics devices & efficient controls in renewable power systems.

Jiexian Mao received his master's degree in 2017. He studied in the field of new energy science and technology. During the study, he participated in 2 research projects at provincial and ministerial level, got 2 intellectual property rights such as patent and soft book, and got 2 awards in competitions above provincial level.